ARTICLE

ACS chemical biology

Site-Activated Chelators Targeting Acetylcholinesterase and Monoamine Oxidase for Alzheimer's Therapy

Hailin Zheng[†,§], Moussa B. H. Youdim[‡,*], and Mati Fridkin[†,*]

[†]Department of Organic Chemistry, The Weizmann Institute of Science, Rehovot 76100, Israel, [‡]Eve Topf and USA National Parkinson Foundation Centers of Excellence for Neurodegenerative Diseases and Department of Pharmacology, Technion-Rappaport Family Faculty of Medicine Haifa, 31096, Israel, and [§]Current address: Department of Medicinal Chemistry, Intra-cellular Therapies Inc., 3960 Broadway, New York, New York 10032

ABSTRACT Chelators have the potential to treat the underlying cause of Alzheimer's disease (AD), but their therapeutic use is hampered by their poor targeting and poor permeability to the brain and/or toxic effects. Here, we report a new strategy for designing site-activated chelators targeting both acetylcholinesterase (AChE) and monoamine oxidase (MAO). We demonstrated that our lead **2** inhibited both AChE and MAO *in vitro*, but with little affinity for metal (Fe, Cu, and Zn) ions. Compound **2** can be activated by inhibition of AChE to release an active chelator **M30**. **M30** has been shown to be able to modulate amyloid precursor protein regulation and β-amyloid reduction, suppress oxidative stress, and passivate excess metal ions (Fe, Cu, and Zn). Compound **2** was less cytotoxic and more lipophilic than the brain-permeable chelator **M30**. Our new strategy is relatively simple and generally produces small and simple molecules with drug-like properties; it thus holds a potential use in designing site-activated multifunctional chelators with safer and more efficacious properties for treating other metal-related diseases such as Parkinson's disease and cancer where specific elimination of metals in cancer cells is required.

Biometal (Fe, Cu, and Zn) levels are increased from 3- to 5-fold in the brains of Alzheimer's disease (AD) compared to those in age-matched controls. They are significantly concentrated in and around β-amyloid (Aβ) plaques and/or neurofibrillary tangles (NFTs) (*1*). Iron closely regulates expression of the Alzheimer's amyloid precursor holo-protein (APP) through an iron-responsive element (IRE) in their APP mRNA 5′ untranslated regions (UTRs); it increases the production of APP translation *via* activation of APP mRNA IRE and consequently Aβ formation (*2, 3*). Biometal (Fe, Cu, and Zn) dyshomeostasis and their interactions with Aβ cause Aβ aggregation and deposition. Iron and copper participate in the Fenton reaction, producing reactive oxygen species (ROS), which aggravates oxidative stress (OS) contributing to tau hyperphosphorylation and NFT formation (*1, 4*). Studies have shown that chelators can block ROS formation, inhibit Aβ aggregation induced by metal ions (Cu, Zn), and partially solubilize Aβ deposits in AD. Chelators possess the potential to attenuate a wide range of OS-related neuropathologies, as well as APP translation, Aβ generation, and amyloid plaques and NFT formation. They are therefore considered as very promising drugs for fighting AD (*5, 6*). Some chelators including clioquinol and desferroxiamine have achieved relative success in transgenic mice and in clinical trials (*7*–*9*). However, these chelators are not designed to selectively target the biometals in the brain. Their therapeutic use is limited by their poor targeting and poor permeability to the brain and/or toxic effects (*10, 11*). Long-term use of strong chelators with poor targeting likely interacts with beneficial biometal and affects the normal physiological functions of

*Corresponding authors, fridkin@weizmann.ac.il, youdim@ tx.technion.ac.il.

Received for review November 27, 2009 and accepted May 7, 2010.

Published online May 10, 2010

10.1021/cb900264w

essential metal-requiring metalloenzymes. To overcome the poor targeting, chelators have been designed as prodrugs or with a neutral amino acid carrier (*12–14*); to enhance the efficacy, chelators have been designed to include antioxidant and/or monoamine oxidase A/B inhibitory activity or amyloid binding property (*13, 15–18*).

AD is a complex disorder with various pathologies and various cascades of molecular events, where the present treatments offer at best moderate symptomatic benefit without arresting the disease progression. Because of the complex etiology of AD, new approaches that simultaneously hit multiple targets involved in AD pathologies are therefore considered as promising strategies for effectively treating AD (*6, 19–22*). The multifunctional drugs under development for AD include dual inhibitors of acetylcholinesterase (AChE)-monoamine oxidase (MAO), or AChE-Aβ aggregation, and metal chelators with antioxidant/amyloid binding properties (*16, 20*).

MAO-B activity increases with age and is particularly high around the senile plaques (SP) in AD patients (*23*). This increase in MAO-B activity results in an elevation of brain levels of neurotoxic free radicals, which further aggravates oxidative stress. Oxidative stress occurs significantly before the development of SP and NFT and serves to increase Aβ and tau hyperphosphorylation (*4, 24*). Inhibition of MAO A/B increases the levels of neurotransmitters such as dopamine, noradrenalin, and serotonin in the CNS (*25*). These neurotransmitters are decreased in AD patients compared to age-matched controls (*26*). Selegiline, a selective MAO-B inhibitor, has been shown to significantly improve learning and memory deficits in animal models associated with AD and to slow the disease progression in AD patients (*27*). In addition, selegiline combined with AChE inhibitor physostigmine (or tacrine) in treating AD patients has shown possible synergistic effects (*28*). These synergistic effects are more significant with Ladostigil, a dual inhibitor of ChE-MAO A/B, which is currently in phase II clinical trials for treating AD and other forms of dementia (*29*).

Recently we reported a site-activated chelator-AChE inhibitor **HLA20A** (*30*). Here we present a new class of site-activated chelators with dual AChE-MAO inhibitory activities. These new prochelators would have several advantages over currently available prochelators or chelators: first, they would act as **HLA20A** to selectively inhibit AChE with little metal ion binding affinity. Second, compared with **HLA20A**, these new prochelators would possess additional activity against MAO A/B. Third, they would be activated by AChE, which is mainly located in the brain, to release an active chelator **M30**. Previous studies have shown that **M30** is a neuroprotective chelator with the capacities of modulating APP regulation, Aβ reduction, and inhibiting Aβ aggregation induced by metal (Cu and Zn) ion (*6, 31*). **M30** is also a potent brain selective MAO-A and -B inhibitor and a strong metal (Fe, Cu, and Zn) chelator with activities against oxidative stress, metal toxicity, and metal dyshomeostasis in the brain (*15, 17, 18, 32*). In this paper we described the rational design, synthesis, and *in vitro* evaluation of two such new compounds (Chart 1): 5-(*N*-methyl-*N*-propargyl-aminomethyl) quinolin-8-yl dimethyl carbamate (**2**) and 5-(*N*-methyl-*N*-propargylaminomethyl) quinolin-8-yl ethylmethyl carbamate (**3**).

Chart 1. Strategy for site-activated chelators targeting both AChE and MAO

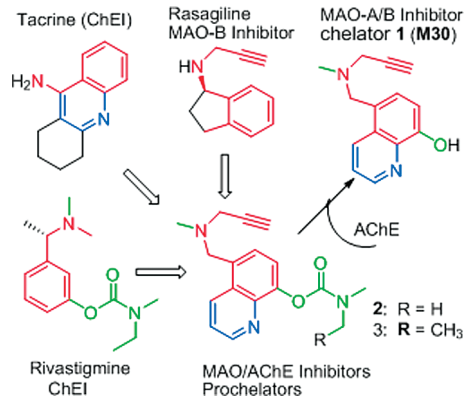

RESULTS AND DISCUSSION

Drug Design. The rational design started from tacrine, rivastigmine, and rasagiline. We selected them as the starting leads for three reasons. First, tacrine and rivastigmine are two AChE inhibitors approved by FDA for treating AD in the clinic. Second, rasagiline (Azilect), which was discovered in our laboratory, is a novel second-generation, selective MAO-B inhibitor, a FDA-approved drug for treating early Parkinson's disease or more advanced PD with levodopa; furthermore, rasagiline may have the potential to slow the neurodegeneration (*33*). Third, the propargylamine moiety in the structure of rasagiline is a neuroprotective and

SCHEME 1. Synthesis of prochelators 2 and 3

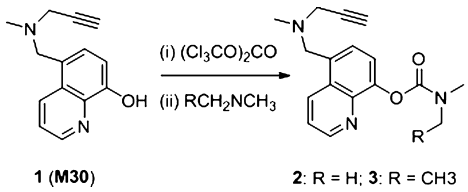

neurorestorative moiety responsible not only for MAO-A/B inhibitory profile but also for APP processing (which helps reduce the SP formation) and for increase in nerve growth factor (*34, 35*). Using the pharmacophoric moieties in the three drugs as building blocks, we reconstructed our drug candidates by highly merging the underlying pharmacophores (Chart 1). One of the advantages of our strategy is to give rise to small and simple molecules with better drug-like properties and high probability of crossing the blood–brain barrier (BBB). The novelty of our strategy is that the multifunctional chelator **M30** has been merged in these new compounds as prochelators.

Drug Synthesis. New prochelators **2** and **3** were synthesized by one-pot, two-step reaction as shown (Scheme 1). The synthesis started from 5-(*N*-methyl-*N*-propargylaminomethyl)-8-hydroxylquinoline (**M30**), which was prepared as described previously (*18*). The treatment of **M30** with triphosgene followed by coupling to dimethylamine or ethyl-methylamine produced crude compounds **2** and **3**, respectively, which were purified by HPLC and characterized by LC–MS, ^{1}H NMR, and ^{13}C NMR (see Supporting Information).

Inhibition of ChE *in Vitro*. A modified Ellman's method (see Supporting Information) was employed to

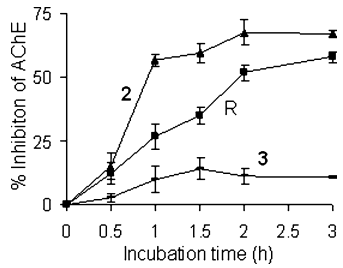

Figure 1. Time-course of AChE inhibitions by 2, 3, and rivastigmine at 1 μM. The inhibitions were determined by a modified Ellman method. Data are means ± SEM of 3–5 independent experiments each done in triplicate.

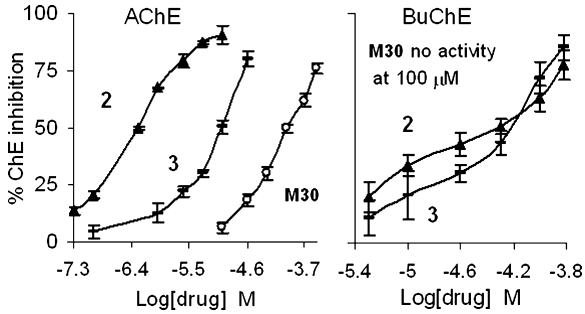

Figure 2. Inhibition of AChE and BuAChE in rat brain homogenates by 2, 3, and M30 at various concentrations. The inhibition was determined by a modified Ellman method after preincubations of the enzymes with 2, 3, or M30 for 3 h, using acetylthiocholine as a substrate for AChE and butyrylthiocholine for BuAChE. Data are means ± SEM of 3–5 independent experiments each done in triplicate. The IC_{50} values were calculated by nonlinear curve.

determine the inhibition of **2** and **3** against AChE and BuChE in rat brain homogenate, using rivastigmine as a reference. Figure 1 shows the time-course of AChE inhibition by **2**, **3**, and rivastigmine at 1 μM, indicating that both **2** and **3** act like rivastigmine to progressively inhibit AChE as the incubation time increases. Compound **2** was more potent, but **3** less potent, than rivastigmine in inhibiting AChE at 1 μM. The IC_{50} values of **2** and **3** against AChE and BuChE activity, calculated from the ChE inhibition curves (Figure 2), were 0.52 ± 0.07 μM (AChE), 44.90 ± 6.10 μM (BuChE) for **2** and 9.80 ± 0.55 μM (AChE), 60.73 ± 5.33 (BuChE) for **3**. The selectivity of **2** and **3** toward AChE (IC_{50} BuChE/IC_{50} AChE) = 86.35 and 6.20, respectively. For comparison, the inhibition of the activated chelator **M30** against AChE and BuChE in rat brain homogenate was also determined. It was found that **M30** was a weak AChE inhibitor with an IC50 value of 113.86 ± 14.05 μM and without significant inhibition of BuChE at 100 μM (Figure 2).

Inhibition of MAO *in Vitro*. The inhibition of MAO by **2** and **3** was determined in rat brain homogenate using the activated chelator **M30** as control. As shown (Figure 3), **2** and **3** were very effective in inhibiting MAO-A with IC_{50} values of 0.0077 ± 0.0007 and 0.0096 ± 0.0005 μM, respectively. They were about 3-fold more potent in inhibiting MAO-A than **M30**. By contrast, **2** was much less effective in inhibiting MAO-B than **M30** (IC_{50} value of 7.90 ± 1.34 μM for **2** versus

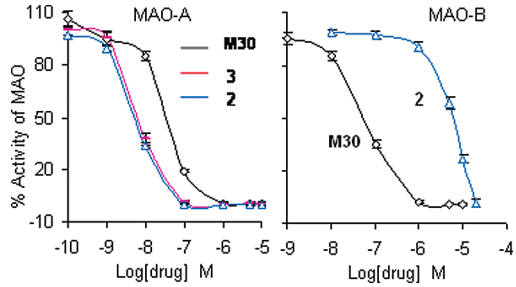

Figure 3. Concentration-dependent inhibittion of rat brain MAO by 2, 3, **and** M30**. Rat brain homogenates were incubated with drugs in the presence of 0.05 μM deprenyl (for the assay of MAO-A) or 0.05 μM clorgyline (for the assay of MAO-B) for 1 h. This was followed by 30 min of incubation with ^{14}C-5-hydroxy-tryptamine or 20 min with ^{14}C-β-phenylethylamine, respectively. The results are the mean SEM, $n = 3$ in triplicates.**

0.037 ± 0.02 μM for **M30**), and **3** showed only minor inhibitory effect on MAO-B with 9% inhibition at 10 μM.

Metal Ions Binding Studies. Prochelator **2**, which is more potent than rivastigmine in inhibiting AChE *in vitro*, was selected for further studies. To examine whether **2** can chelate metal (Fe, Cu, and Zn) ions, UV–vis spectroscopy was used. As seen in Figure 4, panels b or c, no new bands in the UV−vis region appeared upon the addition of $ZnCl_2$ or $CuSO_4$ to a solution of **2**, suggesting little or no complexation between **2** and Zn^{2+}or Cu^{2+}. Addition of $FeCl_3$ or $FeSO_4$ to a solution of **2** led to a slight increase at 292 nm and a shoulder at around 345 nm (Figure 4, panels e and d), which may indicate a weak interaction. It is known that 8-Quinolinol-Fe complex derivatives have two characteristic absorption bands at around 460 and 590 nm. The absence of such new characteristic bands suggests that stable com-

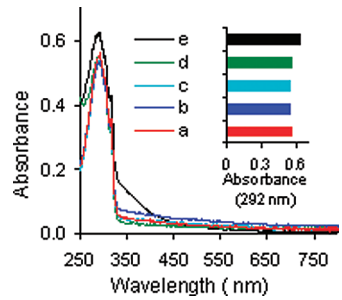

Figure 4. Changes in absorbance of 2 **(0.1 mM in 5%NH_4Ac, pH = 7) on addition of metal salts (0.1 mM): a)** 2**, b)** 2 **+ $ZnCl_2$, c)** 2 **+ $CuSO_4$, d)** 2 **+ $FeSO_4$, e)** 2 **+ $FeCl_3$. Inset: absorbance spectra at 292 nm.**

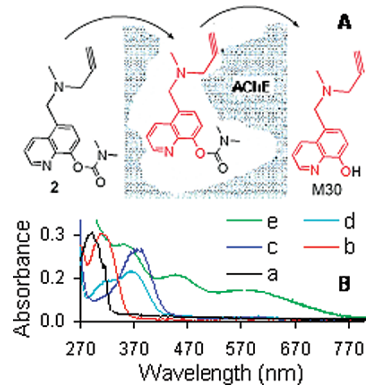

Figure 5. A) Prochelator strategy to release an active chelator M30 **by inhibition of AChE. B) UV–vis absorption spectra of** 2 **and** M30 **(0.1 mM in 5% NH_4Ac, pH = 7) in the absence and presence of metal salts (0.1 mM): a)** 2**; b)** M30**; c)** M30 **+ CuSO4; d)** M30 **+ $ZnCl_2$; e)** M30 **+ $FeSO_4$.**

plexes involving coordination of a sp^2 hydridized nitrogen are not formed in this case.

Prochelator Activation *in Vitro*. To test whether **2** can be activated to **M30** by enzymatic removal of its carbamyl moiety, we used an AChE-mediated hydrolysis model. As shown (Figure 5), the UV–vis spectrum of **2** exhibited a maximal absorbance at 283 nm (black line). This absorbance was shifted to 305 nm (red line) upon activation by AChE. The band at 305 nm disappeared, and new bands appeared (Figure 5, blue, yellow, and green lines) when metal ion salts were added to an extract from a solution of AChE-activated **2**. These results suggest that AChE was activated **2** to **M30**, which reacted with metal (Fe, Cu, and Zn) ions and formed metal–**M30** complexes. The mass spectrometry analysis of the extract showed a value of *m*/*z* 227.22, corresponding to *m*/*z* of [**M30** + H]$^+$, which confirms that **2** was converted to **M30**.

Effects of Procreator and Chelator on Cell Viability. Procreator **2** and its activated chelator **M30** were tested for their effects on human SH-SY5Y neuroblastoma cells. After exposure to **2** or **M30** for 48 h, the cell viability was measured by 3-(4.5-dimethylthiazol-2-yl)-2.5-diphenyltetrazolium (MTT) assay. As shown (Figure 6), both **2** and **M30** did not significantly modify the cell viability at 1 μM. However, at higher concentrations, **2** showed much lower toxicity to the cells compared to **M30** (16%, 25%, and 16% increase in cell viability at 10, 25, and 50 μM, respectively).

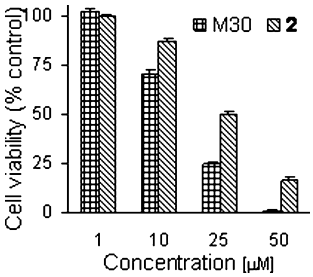

Figure 6. Assessment of the cytotoxicity of M30 **and** 2**. Human SH-SY5Y neuroblastoma cells were exposure to** M30 **and** 2 **for 48 h, and the cell viability was tested by MTT assays (see Supporting Information for details). Data are means ± SEM of three independent experiments.**

Discussion. Simultaneous modulation of multiple targets related to AD etiology holds a promise for effectively treating the now incurable AD (*6, 13, 19–22*). In this paper we have described a new class of site-activated chelators with dual inhibition of AChE-MAO.

Our results demonstrate that both **2** and **3** act as rivastigmine to inhibit AChE activity in a time-dependent manner and attain maximum inhibition of AChE after **2** h of preincubation (Figure 1). Compound **2** is about 18-fold more potent than **3** and also more potent than rivastigmine against AChE. However, unlike rivastigmine as a potent BuChE inhibitor, both **2** and **3** display only minor inhibition of BuChE activity. Compound **2** shows high selectivity toward AChE (Figure 2). It is known that the ethyl carbamates are generally less potent than their methyl analogues against AChE because of a steric hindrance effect between the ethyl moiety and His440 in the AChE active site (*36*). This may partly explain the lower potency of the ethyl carbamate **3** against AChE compared to its methyl carbamate analogue **2**. Recently, BuChE has also been proposed as a potential target for AD treatment, as it may play an important role in the metabolism of AChE in the central nervous system (CNS) (*37*). However, studies also pointed out that BuChE activity is not increased in AD synapses, which does not support targeting BuChE for preventing increased levels of BuChE from metabolizing acetylcholine in AD cerebral cortex (*38*). As with our prochelator **2**, its high selectivity toward AChE with weak inhibition of BuChE may offer additional advantages over nonselective AChE inhibitors. First, it may help minimize toxic effects commonly associated with the use of nonselective AChE inhibitors such as tacrine, its hepatotoxicity likely attributed to its poor selectivity for AChE (*39*). Second, as BuChE predominates over AChE in the peripheral system, the weak inhibition of BuChE may minimize the possibility of BuChE-mediated cleavage of **2** to the strong metal chelator **M30** before entering the CNS, thus improving its target specificity. In addition, studies also suggest that patients with BuChE deficiency may not tolerate AChE inhibitor drugs such as donepezil, as BuChE also functions in neurotransmission (*40*).

MAO-A inhibitors as antidepressants have high mood-enhancing efficacy and advantages over other antidepressants for treating resistant depression, dysthymia, and atypical depression (*41*). However, irreversible inhibition of MAO-A in liver and intestine is associated with the cheese effect (potentiation of tyramine-induced hypertension) (*41*). Brain selective or reversible inhibition of MAO-A does not induce the cheese effect at their therapeutic dosage, as evidenced by moclobemide (reversible MAO-A inhibitor) and transdermal selegiline (irreversible brain selective MAO-A and -B inhibitor) (*42, 43*). Both **2** and **3** exhibit very potency against MAO-A with weak inhibition of MAO-B *in vitro*. This is in contrast with their activated chelator **M30**, which shows potency against both MAO-A and -B *in vitro* (IC_{50}: MAO-A, 0.037 ± 0.02; MAO-B, 0.057 ± 0.01) (*17*). In *in vivo* studies, however, **M30** displays strong brain-selective inhibition of both MAO-A and -B with little or no inhibition of these enzymes in the liver and intestine (*15*). Studies have also shown that **M30** raises striatal levels of dopamine, noradrenaline, and serotonin and induces limited cheese effect, similar to ladostigil, and the selective reversible MAO-A inhibitor antidepressant moclobemide (*44*). Whether **2** and/or **3** *in vivo* behave like **M30** to selectively inhibit MAO-A and/or -B in the brain is not clear yet.

Chelators for clinical use in neurological disorders should (i) pass the BBB to selectively target metal toxicity in the brain, (ii) chelate the disease-related metals in the CNS without significant disruption of healthy metal homeostasis in the body, and (iii) possess adequate affinity for metal ions so as to be able to remove the disease-related metals in the brain. Increasing the lipophilicity of a chelator may improve its penetration into not only the brain but also other nonrelated tissues (cells) in the body; this will potentially induce side effects as seen with traditional chelators, especially when administered for prolonged periods of time (*10, 11*). Compound **2** is a small and simple molecule with more lipophilic than its activated chelator **M30**, as sug-

gested by the calculated log *P* (log *P* value of 2.0 for **2** versus 1.89 for **M30**). As **M30** has been shown to be able to cross the BBB *in vivo* (*15*), it is possible that **2** acts as **M30** to penetrate into the brain *in vivo*. Our *in vitro* experiments indicate that **2** at high concentrations is much less toxic than its activated chelator **M30** (Figure 6), substantiating our prochelator strategy for minimizing toxicity related to the use of traditional chelators. Compound **2** is found to be readily converted to its OH-metabolite **M30** by AChE (Figure 5). This finding is consistent with the previous reports that carbamate AChE inhibitors such as rivastigmine and rasagiline are readily hydrolyzed by AChE *in vivo* with a concomitant release in the brain of their OH-metabolites (*45*). The OH-metabolite **M30** is a strong chelator with the capacity to chelate metal ions *in vitro* (Figure 5) (*18*) and to attenuate lactacystin-induced iron accumulation in the brain *in vivo* (*32*).

Neuroprotective effects of chelators are believed to be *via* metal chelation, resulting in Aβ dissolution (*5*). Additionally, chelators may also promote neuroprotection by activating neuroprotective cell signaling pathways. Central to these pathways is inhibition of glycogen synthase kinase 3β (GSK-3β) (*46*). Recent studies have shown that clioquinol, an 8-hydroxyquinoline containing chelator like **M30**, is able to chelate Cu and Zn from both amyloid plaques and the synaptic cleft and act as an ionophore to enhance intracellular Cu and Zn uptake. The increase in intracellular copper level is proposed to inhibit GSK-3β through activation of an Akt (protein kinase B) signaling pathway. This results in a substantial decrease in tau phosphorylation and attenuation of cognitive deficits (*46, 47*). **M30** was recently found to increase the levels of phospho-AKT (Ser473) and phospho-GSK-3β (Ser9) and reduce tau phosphorylation. **M30** also activates the hypoxia-inducible factor (HIF)-1α signaling pathway, thus promoting HIF-1α mRNA and protein expression levels, as well as enhancing transcription of HIF-1α-dependent genes, including vascular endothelial growth factor, erythropoietin, enolase-1, p21, and tyrosine hydroxylase in rat primary cortical cells (*48, 49*).

In summary, we have demonstrated the feasibility of our strategy for rationally designing a new class of site-activated chelators with dual inhibition of AChE and MAO-A/B. Compared with traditional lead discovery strategies, our strategy requires only a limited number of compounds to be synthesized and generates small and simple molecules with better drug-like properties and high probability of crossing the BBB. The novelty of our strategy is that the multifunctional chelator **M30** has been merged in these new compounds as prochelators. Our lead **2** is a small and simple molecule with low molecular weigh (297 Da) and inhibits both AChE and MAO-A/B activity *in vitro*. It shows much lower cytotoxicity and more lipophilicity than its activated brain-permeable chelator **M30**. Compound **2** has little affinity for metal (Fe, Cu, and Zn) ions but can be activated by inhibition of AChE to release an active chelator **M30**. Therefore, **2** represents a promising lead for further development. In addition, our new strategy may also find application in designing site-activated chelators with safer and more efficacious properties as potential anti-Parkinson and anticancer drugs, conditions in which metal dyshomeostasis are implicated in their pathologies.

METHODS

Synthesis of 2 and 3. Starting material **M30** was prepared as described previously (*18*). Other materials were from Aldrich, Merck, or Fluka. Compounds **2** and **3** were obtained by one-pot, two-step reaction (Scheme 1). The crude products were purified by HPLC, and their structures were confirmed by LC–MS, ^{1}H NMR, and ^{13}C NMR (see Supporting Information for details).

Determination of Inhibition of AChE and BChE Activity. Ellman's method was adapted for determination of AChE and BuAChE activities in rat brain homogenates. The assay was performed in 96-well microplates and was followed at 412 nm for 5 min with a plate reader. Results are reported as mean (SEM of IC_{50} obtained independently from 3−5 experiments (see Supporting Information for details).

Cytotoxicity Assays. Human SH-SY5Y neuroblastoma cells were exposed to drugs for 48 h, and the cell viability was tested by MTT assays (see Supporting Information for details).

Prochelator Activation *in Vitro*. Compound **2** was incubated with an excess of AChE from *Electrophorus electricus* (electric eel) (Sigma) for 1 h; the metabolite **M30** was extracted using ethyl acetate and checked by LC–MS (see Supporting Information for details).

Acknowledgment: We thank the Alzheimer Association (USA), Alzheimer Drug Discovery Foundation (New York, USA), Technion-Research and Development, and the Weizmann Institute for generous support of this work.

Supporting Information Available: This material is available free of charge *via* the Internet at http://pubs.acs.org.

REFERENCES

1. Barnham, K. J., and Bush, A. I. (2008) Metals in Alzheimer's and Parkinson's diseases, *Curr. Opin. Chem. Biol. 12*, 222–228.

2. Bandyopadhyay, S., Huang, X., Cho, H., Greig, N. H., Youdim, M. B., and Rogers, J. T. (2006) Metal specificity of an iron-responsive element in Alzheimer's APP mRNA 5′untranslated region, tolerance of SH-SY5Y and H4 neural cells to desferrioxamine, clioquinol, VK-28, and a piperazine chelator, *J. Neural Transm. Suppl. 237*–247.
3. Rogers, J. T., Randall, J. D., Cahill, C. M., Eder, P. S., Huang, X., Gunshin, H., Leiter, L., McPhee, J., Sarang, S. S., Utsuki, T., Greig, N. H., Lahiri, D. K., Tanzi, R. E., Bush, A. I., Giordano, T., and Gullans, S. R. (2002) An iron-responsive element type II in the 5′-untranslated region of the Alzheimer's amyloid precursor protein transcript, *J. Biol. Chem. 277*, 45518–45528.
4. Sayre, L. M., Perry, G., and Smith, M. A. (2008) Oxidative stress and neurotoxicity, *Chem. Res. Toxicol. 21*, 172–188.
5. Bolognin, S., Drago, D., Messori, L., and Zatta, P. (2009) Chelation therapy for neurodegenerative diseases, *Med. Res. Rev. 29*, 547–570.
6. Amit, T., Avramovich-Tirosh, Y., Youdim, M. B., and Mandel, S. (2008) Targeting multiple Alzheimer's disease etiologies with multimodal neuroprotective and neurorestorative iron chelators, *FASEB J. 22*, 1296–1305.
7. Adlard, P. A., Cherny, R. A., Finkelstein, D. I., Gautier, E., Robb, E., Cortes, M., Volitakis, I., Liu, X., Smith, J. P., Perez, K., Laughton, K., Li, Q. X., Charman, S. A., Nicolazzo, J. A., Wilkins, S., Deleva, K., Lynch, T., Kok, G., Ritchie, C. W., Tanzi, R. E., Cappai, R., Masters, C. L., Barnham, K. J., and Bush, A. I. (2008) Rapid restoration of cognition in Alzheimer's transgenic mice with 8-hydroxy quinoline analogs is associated with decreased interstitial Aβ, *Neuron 59*, 43–55.
8. Crapper McLachlan, D. R., Dalton, A. J., Kruck, T. P., Bell, M. Y., Smith, W. L., Kalow, W., and Andrews, D. F. (1991) Intramuscular desferrioxamine in patients with Alzheimer's disease, *Lancet 337*, 1304–1308.
9. Kaur, D., Yantiri, F., Rajagopalan, S., Kumar, J., Mo, J. Q., Boonplueang, R., Viswanath, V., Jacobs, R., Yang, L., Beal, M. F., DiMonte, D., Volitaskis, I., Ellerby, L., Cherny, R. A., Bush, A. I., and Andersen, J. K. (2003) Genetic or pharmacological iron chelation prevents MPTP-induced neurotoxicity *in vivo*: a novel therapy for Parkinson's disease, *Neuron 37*, 899–909.
10. Arasaki, K., and Nakanishi, T. (1989) Selective neurotoxicity of clioquinol on the function of the posterior column nuclei, *Neurosci. Lett. 107*, 85–88.
11. Porter, J. B., and Huehns, E. R. (1989) The toxic effects of desferrioxamine, *Bailliere's Clin. Haematol. 2*, 459–474.
12. Charkoudian, L. K., Pham, D. M., and Franz, K. J. (2006) A prochelator triggered by hydrogen peroxide inhibits iron-promoted hydroxyl radical formation, *J. Am. Chem. Soc. 128*, 12424–12425.
13. Schugar, H., Green, D. E., Bowen, M. L., Scott, L. E., Storr, T., Bohmerle, K., Thomas, F., Allen, D. D., Lockman, P. R., Merkel, M., Thompson, K. H., and Orvig, C. (2007) Combating Alzheimer's disease with multifunctional molecules designed for metal passivation, *Angew. Chem., Int. Ed. 46*, 1716–1718.
14. Zheng, H., Youdim, M. B., Weiner, L. M., and Fridkin, M. (2005) Novel potential neuroprotective agents with both iron chelating and amino acid-based derivatives targeting central nervous system neurons, *Biochem. Pharmacol. 70*, 1642–1652.
15. Gal, S., Zheng, H., Fridkin, M., and Youdim, M. B. (2005) Novel multifunctional neuroprotective iron chelator-monoamine oxidase inhibitor drugs for neurodegenerative diseases. *In vivo* selective brain monoamine oxidase inhibition and prevention of MPTP-induced striatal dopamine depletion, *J. Neurochem. 95*, 79–88.
16. Rodriguez-Rodriguez, C., Sanchez de Groot, N., Rimola, A., Alvarez-Larena, A., Lloveras, V., Vidal-Gancedo, J., Ventura, S., Vendrell, J., Sodupe, M., and Gonzalez-Duarte, P. (2009) Design, selection, and characterization of thioflavin-based intercalation compounds with metal chelating properties for application in Alzheimer's disease, *J. Am. Chem. Soc. 131*, 1436–1451.
17. Zheng, H., Gal, S., Weiner, L. M., Bar-Am, O., Warshawsky, A., Fridkin, M., and Youdim, M. B. (2005) Novel multifunctional neuroprotective iron chelator-monoamine oxidase inhibitor drugs for neurodegenerative diseases: *invitro* studies on antioxidant activity, prevention of lipid peroxide formation and monoamine oxidase inhibition, *J. Neurochem. 95*, 68–78.
18. Zheng, H., Weiner, L. M., Bar-Am, O., Epsztejn, S., Cabantchik, Z. I., Warshawsky, A., Youdim, M. B., and Fridkin, M. (2005) Design, synthesis, and evaluation of novel bifunctional iron-chelators as potential agents for neuroprotection in Alzheimer's, Parkinson's, and other neurodegenerative diseases, *Bioorg. Med. Chem. 13*, 773–783.
19. Bolognesi, M. L., Matera, R.,, Minarini, A., Rosini, M., and Melchiorre, C. (2009) Alzheimer's disease: new approaches to drug discovery, *Curr. Opin. Chem. Biol 13*, 303–308.
20. Cavalli, A., Bolognesi, M. L., Minarini, A., Rosini, M., Tumiatti, V., Recanatini, M., and Melchiorre, C. (2008) Multi-target-directed ligands to combat neurodegenerative diseases, *J. Med. Chem. 51*, 347–372.
21. Frantz, S. (2005) Drug discovery: playing dirty, *Nature 437*, 942–943.
22. Schrattenholz, A., and Soskic, V. (2008) What does systems biology mean for drug development? *Curr. Med. Chem. 15*, 1520–1528.
23. Saura, J., Luque, J. M., Cesura, A. M., Da Prada, M., Chan-Palay, V., Huber, G., Loffler, J., and Richards, J. G. (1994) Increased monoamine oxidase B activity in plaque-associated astrocytes of Alzheimer brains revealed by quantitative enzyme radioautography, *Neuroscience 62*, 15–30.
24. Nunomura, A., Perry, G., Aliev, G., Hirai, K., Takeda, A., Balraj, E. K., Jones, P. K., Ghanbari, H., Wataya, T., Shimohama, S., Chiba, S., Atwood, C. S., Petersen, R. B., and Smith, M. A. (2001) Oxidative damage is the earliest event in Alzheimer disease, *J. Neuropathol. Exp. Neurol. 60*, 759–767.
25. Youdim, M. B., Edmondson, D., and Tipton, K. F. (2006) The therapeutic potential of monoamine oxidase inhibitors, *Nat. Rev. Neurosci. 7*, 295–309.
26. Reinikainen, K. J., Soininen, H., and Riekkinen, P. J. (1990) Neurotransmitter changes in Alzheimer's disease: implications to diagnostics and therapy, *J. Neurosci. Res. 27*, 576–586.
27. Sano, M., Ernesto, C., Thomas, R. G., Klauber, M. R., Schafer, K., Grundman, M., Woodbury, P., Growdon, J., Cotman, C. W., Pfeiffer, E., Schneider, L. S., and Thal, L. J. (1997) A controlled trial of selegiline, α-tocopherol, or both as treatment for Alzheimer's disease. The Alzheimer's Disease Cooperative Study, *N. Engl. J. Med. 336*, 1216–1222.
28. Schneider, L. S., Olin, J. T., and Pawluczyk, S. (1993) A double-blind crossover pilot study of L-deprenyl (selegiline) combined with cholinesterase inhibitor in Alzheimer's disease, *Am. J. Psychiatry 150*, 321–323.
29. Weinreb, O., Amit, T., Bar-Am, O., Yogev-Falach, M., and Youdim, M. B. (2008) The neuroprotective mechanism of action of the multimodal drug ladostigil, *Front Biosci. 13*, 5131–5137.
30. Zheng, H., Youdim, M. B., and Fridkin, M. (2009) Site-activated multifunctional chelator with acetylcholinesterase and neuroprotective-neurorestorative moieties for Alzheimer's therapy, *J. Med. Chem. 52*, 4095–4098.
31. Avramovich-Tirosh, Y., Amit, T., Bar-Am, O., Zheng, H., Fridkin, M., and Youdim, M. B. (2007) Therapeutic targets and potential of the novel brain-permeable multifunctional iron chelator-monoamine oxidase inhibitor drug, M-30, for the treatment of Alzheimer's disease, *J. Neurochem. 100*, 490–502.
32. Zhu, W., Xie, W., Pan, T., Xu, P., Fridkin, M., Zheng, H., Jankovic, J., Youdim, M. B., and Le, W. (2007) Prevention and restoration of lactacystin-induced nigrostriatal dopamine neuron degeneration by novel brain-permeable iron chelators, *FASEB J. 21*, 3835–3844.

33. Chen, J. J., Swope, D. M., and Dashtipour, K. (2007) Comprehensive review of rasagiline, a second-generation monoamine oxidase inhibitor, for the treatment of Parkinson's disease, *Clin. Ther. 29*, 1825–1849.
34. Bar-Am, O., Weinreb, O., Amit, T., and Youdim, M. B. (2005) Regulation of Bcl-2 family proteins, neurotrophic factors, and APP processing in the neurorescue activity of propargylamine, *FASEB J. 19*, 1899–1901.
35. Weinreb, O., Amit, T., Bar-Am, O., Chillag-Talmor, O., and Youdim, M. B. (2005) Novel neuroprotective mechanism of action of rasagiline is associated with its propargyl moiety: interaction of Bcl-2 family members with PKC pathway, *Ann. N.Y. Acad. Sci. 1053*, 348–355.
36. Bar-On, P., Millard, C. B., Harel, M., Dvir, H., Enz, A., Sussman, J. L., and Silman, I. (2002) Kinetic and structural studies on the interaction of cholinesterases with the anti-Alzheimer drug rivastigmine, *Biochemistry 41*, 3555–3564.
37. Greig, N. H., Utsuki, T., Yu, Q., Zhu, X., Holloway, H. W., Perry, T., Lee, B., Ingram, D. K., and Lahiri, D. K. (2001) A new therapeutic target in Alzheimer's disease treatment: attention to butyrylcholinesterase, *Curr. Med. Res. Opin. 17*, 159–165.
38. Kuhl, D. E., Koeppe, R. A., Snyder, S. E., Minoshima, S., Frey, K. A., and Kilbourn, M. R. (2006) *In vivo* butyrylcholinesterase activity is not increased in Alzheimer's disease synapses, *Ann. Neurol. 59*, 13–20.
39. Patani, G. A., Pang, Y. P., and Chien, Y. W. (2005) A potent and selective tacrine analog–biomembrane permeation and physicochemical characterization, *Pharm. Dev. Technol. 10*, 525–538.
40. Duysen, E. G., Li, B., Darvesh, S., and Lockridge, O. (2007) Sensitivity of butyrylcholinesterase knockout mice to (−)-huperzine A and donepezil suggests humans with butyrylcholinesterase deficiency may not tolerate these Alzheimer's disease drugs and indicates butyrylcholinesterase function in neurotransmission, *Toxicology 233*, 60–69.
41. Bortolato, M., Chen, K., and Shih, J. C. (2008) Monoamine oxidase inactivation: from pathophysiology to therapeutics, *Adv. Drug Delivery Rev. 60*, 1527–1533.
42. Bonnet, U. (2002) Moclobemide: evolution, pharmacodynamic, and pharmacokinetic properties, *CNS Drug Rev. 8*, 283–308.
43. Lee, K. C., and Chen, J. J. (2007) Transdermal selegiline for the treatment of major depressive disorder, *Neuropsychiatr. Dis. Treat. 3*, 527–537.
44. Gal, S., Abassi, Z. A., and Youdim, M. B. (2009) Limited potentiation of blood pressure in response to oral tyramine by the anti-Parkinson brain selective multifunctional monoamine oxidase-AB inhibitor, M30, *Neurotox. Res.* Epub ahead of print, DOI: 10.1007/s12640-009-9128-8.
45. Groner, E., Ashani, Y., Schorer-Apelbaum, D., Sterling, J., Herzig, Y., and Weinstock, M. (2007) The kinetics of inhibition of human acetylcholinesterase and butyrylcholinesterase by two series of novel carbamates, *Mol. Pharmacol. 71*, 1610–1617.
46. White, A. R., Du, T., Laughton, K. M., Volitakis, I., Sharples, R. A., Xilinas, M. E., Hoke, D. E., Holsinger, R. M., Evin, G., Cherny, R. A., Hill, A. F., Barnham, K. J., Li, Q. X., Bush, A. I., and Masters, C. L. (2006) Degradation of the Alzheimer disease amyloid β-peptide by metal-dependent up-regulation of metalloprotease activity, *J. Biol. Chem. 281*, 17670–17680.
47. Price, K. A., Filiz, G., Caragounis, A., Du, T., Laughton, K. M., Masters, C. L., Sharples, R. A., Hill, A. F., Li, Q. X., Donnelly, P. S., Barnham, K. J., Crouch, P. J., and White, A. R. (2008) Activation of epidermal growth factor receptor by metal-ligand complexes decreases levels of extracellular amyloid beta peptide, *Int. J. Biochem. Cell Biol. 40*, 1901–1917.
48. Avramovich-Tirosh, Y., Bar-Am, O., Amit, T., Youdim, M. B., and Weinreb, O. (2010) Up-regulation of hypoxia-inducible factor (HIF)-1α and HIF-target genes in cortical neurons by the novel multifunctional iron chelator anti-Alzheimer drug, M30, *Curr. Alzheimer Res.* Epub ahead of print.
49. Kupershmidt, L., Weinreb, O., Amit, T., Mandel, S., Carri, M. T., and Youdim, M. B. (2009) Neuroprotective and neuritogenic activities of novel multimodal iron-chelating drugs in motor-neuron-like NSC-34 cells and transgenic mouse model of amyotrophic lateral sclerosis, *FASEB J. 23*, 3766–3779.